Journal of Materials Chemistry A

Accepted Manuscript

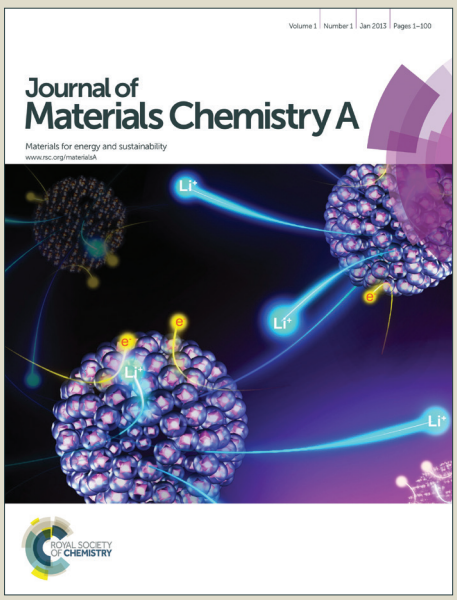

ROYAL SOCIETY OF CHEMISTRY

www.rsc.org/materialsA

The General Synthesis of Ag Nanoparticles Anchored on Silver Vanadium Oxides: Towards High Performance Cathodes for Lithium-ion Batteries

Jiang Zhou,[a] Qiang Liang,[a] Anqiang Pan,[a,] Xuelin Zhang,[a] Qinyu Zhu,[a] Shuquan Liang,[a,]* and Guozhong Cao[b,]**

[a] School of Materials Science and Engineering, Central South University, Changsha 410083, P. R. China

[b] Department of Materials Science & Engineering, University of Washington, UW, 98195, USA

Corresponding authors:

pananqiang@gmail.com; lsq@mail.csu.edu.cn; gzcao@u.washington.edu

A general strategy has been developed for the one-pot synthesis of Ag nanoparticles uniformly anchored on silver vanadium oxides (SVOs) including $AgVO_3$, $Ag_2V_4O_{11}$, $Ag_{0.33}V_2O_5$ and $Ag_{1.2}V_3O_8$. All the resulting Ag/SVOs hybrids demonstrated excellent lithium ion electrochemical intercalation properties due largely to the improved conductivity with introduction of silver nanoparticles, large accessible surface and possible catalytic effects. For instance, the as-prepared Ag/$AgVO_3$ hybrid exhibits superior rate capability with a high discharge capacity of 199 mA h g^{-1} even at a rate of 5 A g^{-1}.

As the most complicated phases among the metal oxides, silver vanadium oxides (SVOs) with a number of phases can be obtained under the variations in reaction conditions and material stoichiometry. SVOs with different ratios of silver, vanadium, and oxygen, may result in subtly different physicochemical properties, such as electrochemical property, sensing property, catalytic activity, optical property, magnetic property, electrical property, and so on.[1-9] In particular, SVOs with variety of oxidation states have found their suitable application in lithium batteries. SVOs as

cathode materials possess high capacity and energy density, compared to the traditional cathode materials, thus attracting many researchers' attentions.[1] SVOs are firstly considered as cathode materials in primary lithium batteries because of their high energy density and unsatisfactory cycling behavior. For example, the $Ag_2V_4O_{11}$ has been commercially used as cathode material in primary lithium battery for the power implantable biomedical device. Very recently, many groups[3, 10-13] have developed the nanostructured $AgVO_3$ to improve the cycling performance and rate capability of $AgVO_3$ material. Other silver vanadium oxides, such as $Ag_{0.33}V_2O_5$ and $Ag_{1.2}V_3O_8$, have also been explored as cathode materials in rechargeable lithium batteries.[6, 14, 15] However, their rate capability and cyclic stability are unsatisfactory and still need further improvement.

It is believed an effective approach to obtain the enhanced electrochemical performance by synthesizing SVOs anchored with silver nanoparticles because of the improved conductivity by the metallic silver.[16] Moreover, the Ag/SVOs hybrid also can find their applications in sensors, catalysts, antibacterial agent, water-based paints, surface-enhanced Raman spectroscopy, etc.[5, 13, 17-21] However, it is difficult to synthesis the Ag nanoparticles anchored on the metal oxides with high oxidation state like SVOs. Moreover, to the best of our knowledge, there is no general strategy to prepare a series of SVOs ($AgVO_3$, $Ag_2V_4O_{11}$, $Ag_{0.33}V_2O_5$ and $Ag_{1.2}V_3O_8$). And to develop a general method for the synthesis of uniform Ag nanoparticles anchored on a series of SVOs is challenging and would be of great interest to the scientific community.

In this work, we have developed a facile and scalable strategy to generally prepare Ag nanoparticles anchored on silver vanadium oxides (SVOs), including $AgVO_3$, $Ag_2V_4O_{11}$, $Ag_{0.33}V_2O_5$ and $Ag_{1.2}V_3O_8$. In brief, the NH_4VO_3 powder reacts with H_2O_2 in the de-ionized water to form a bright-yellow solution first, followed by adding a stoichiometric amount of $AgNO_3$. The resulting

homogeneous solution is dried to get the solid precursors, which were further calcined in air at various temperatures to obtain final products. Various silver vanadium oxides ($AgVO_3$, $Ag_2V_4O_{11}$, $Ag_{1.2}V_3O_8$, $Ag_{0.33}V_2O_5$) can be fabricated by tuning the ratio of V to Ag. The detailed experimental sections can be found in the supporting information. The as-synthesized Ag/SVOs hybrids exhibit enhanced electrochemical properties. For examples, a high specific discharge capacity of 199 mA h g^{-1} can still be delivered for the Ag/$AgVO_3$ hybrid even at an ultra-high discharge current density of 5 A g^{-1}. And the rechargeable Ag/$Ag_{0.33}V_2O_5$ hybrid electrode shows remarkable capacity retention of 96.4 % after 200 cycles at 300 mA g^{-1}.

The $AgVO_3$ oxides have three typical crystallographic forms: α-$AgVO_3$, β-$AgVO_3$ and γ-$AgVO_3$.[22] However, α-$AgVO_3$ is metastable, which will irreversibly transform into stable β-$AgVO_3$ phase at around 200 ^oC, and the fabrication of γ-$AgVO_3$ always requires high temperatures.[23] β-$AgVO_3$ is structured of a strong three dimensional network of V_4O_{12} double chains held together by AgO_6 octahedra and firmly interconnected by Ag_2O_5 and Ag_3O_5 square pyramids.[22, 24] Not only the structural stability, but also the peculiar physicochemical properties of the stable phase of β-$AgVO_3$ attract increasing attention in recent years. In our work, the Ag anchored β-$AgVO_3$ in the monoclinic system of the space group of $I2/m(12)$ can be synthesized at a wide temperature. The TG-DSC results suggest that the Ag/$AgVO_3$ hybrid can be readily synthesized at 350 ^oC (Supporting information, Figure S1) because of no obvious peaks have been detected between 329 ^oC and 468 ^oC. The consumption has been confirmed by the XRD patterns shown in Figure 1a. All diffraction peaks in the XRD patterns can be well indexed as monoclinic β-$AgVO_3$ phase (JCPDS card NO. 29-1154)[2, 5, 8] and no new phases are generated between the temperature range. XPS techniques are further employed to study the β-$AgVO_3$ phase (Supporting

information, Figure S2). It is interesting to find the Ag 3d region can be divided into two components of the two peaks of Ag 3d (5/2) and Ag 3d (3/2), indicating the presence of different valence states for the silver species (Figure 1b). The two strong peaks at the Ag region of 367.4 and 373.4 eV can be assigned to Ag^+ Ag3d (5/2) and Ag3d (3/2), respectively, while the two relatively weak peaks located at 368.4 and 374.4 eV can be attributed to Ag^0 Ag3d (5/2) and Ag3d (3/2).[11] The results demonstrate the co-existence of Ag^0 and $AgVO_3$ (Ag^+) in the obtained materials. Recently, many groups have reported can result in a significant increase in conductivity, leading to enhanced electrochemical performance as cathode materials for lithium ion batteries.[16, 25, 26]

The synthesized β-$AgVO_3$ is of rod-like shape with a diameter around 200-500 nm, and many white nanoparticles are anchored on the surface of the material (Supporting information, Figure S3). The detailed structures are revealed by TEM and the results are shown in Figure 1c and 1d. A large number of nanoparticles are uniformly distributed on the surface of $AgVO_3$ nanorod. The diameter of an individual nanoparticle is less than 20 nm. The corresponding High-resolution transmission electron microscopy (HRTEM) (Figure 1d) image confirms that the nanoparticles are Ag nanoparticles, for the clear lattice spacing of ≈ 0.236 nm corresponding well to the lattice spacing of (111) plane for cubic Ag phase [JCPDS card NO. 04-0783]. In addition, the marked d-spacing of ≈ 0.276 nm and ≈ 0.305 nm of the lattice fringes correspond to the distances of (-411) and (310) planes of monoclinic β-$AgVO_3$ phase. The results correspond well with the previous XPS result, which confirms the existence of Ag phase. It is safe to believe that the Ag/$AgVO_3$ hybrid has been successfully prepared by our simple synthesis approach.

The Ag/$AgVO_3$ hybrid calcined at 400 ^oC in air for 4 h are assembled into coin-cells to evaluate their electrochemical properties. Figure 2a shows the initial cyclic voltammetry (CV) curve

of for $Ag/AgVO_3$ hybrid. Three strong cathodic peaks at 2.97, 2.32, and 2.16 V vs. Li/Li^+ and one weak cathodic peak at 1.95 V vs. Li/Li^+ are clearly observed. All the cathodic peaks are associated with the continuous reduction of Ag^+ to Ag^0, the cathodic peaks at 2.32, and 2.16 V vs. Li/Li^+ are attributed to the reduction of V^{5+} to V^{4+} and partial reduction of V^{4+} to V^{3+}, respectively.[11, 12, 22, 27, 28] The weak cathodic peak at 1.95 V vs. Li/Li^+ may be ascribed to the further reduction of vanadium from V^{4+} to V^{3+}.[29] Figure 2b shows the discharge curves of $Ag/AgVO_3$ hybrid electrodes at different current densities. The electrodes deliver high specific discharge capacities of 325, 269, 259, 244, 227 and 215 mA h g^{-1} at the current densities of 5, 20, 100, 500, 1000 and 2000 mA g^{-1}, respectively. Surprisingly, even at an ultra-high discharge current density of 5000 mA g^{-1}, the hybrid still exhibits a high specific discharge capacity of 199 mA h g^{-1}. It has a capacity retention of 74% when the current density raised from 20 mA g^{-1} to 5000 mA g^{-1} (Supporting information, Figure S4), indicating the superior rate capability for the silver nanoparticles anchored on $AgVO_3$ electrode. The Electrochemical Impedance Spectroscopy measurement was also carried out and the simulation charge-transfer resistance is 117 Ω, which is much smaller than those reported for other $AgVO_3$ electrodes, including $AgVO_3$/PANI triaxial nanowires,[10] $Ag/AgVO_3$ hybrid nanorods,[12] polyaniline-coated β-$AgVO_3$ nanowires.[30] The smaller charge-transfer resistance may be due to high electronic conductivity of the as-prepared hybrid electrode, resulting in faster electron transportation. The excellent rate capability of $Ag/AgVO_3$ hybrid can be attributed to the following possible mechanisms: (1) Ag nanoparticles anchored on $AgVO_3$ nanorods and the in-situ generated Ag from $AgVO_3$ during the discharge process (Supporting information, Figure S5) result in the enhanced electron conductivity, (2) ample space between the nanostructured materials would facilitate the electrolyte penetration, and (3) the Ag nanoparticles may have the catalytic effects to

improve the intercalation/de-intercalation reaction at the surface. As shown in Table S1, many synthetic methods have been exploited to improve the electrochemical properties of SVOs electrodes, and some exactly demonstrate the desirable properties. With compared with the present SVOs electrodes, the rate capability of the as-prepared $Ag/AgVO_3$ hybrid is among the best ever reported (Supporting information, Table S1). We also evaluated its long-term cycling performance. After 200 cycles, the capacity quickly decreased to 50 mA h g^{-1}, which can be attributed to the intrinsic irreversibility of $AgVO_3$ electrodes (Supporting information, Figure S6). The capacity fading is attributed to the irreversible phase transition of crystallites upon cycling (Supporting information, Figure S5). However, the high specific discharge capacity and the excellent rate capability of $Ag/AgVO_3$ hybrid have proven it is a promising cathode candidate in primary lithium batteries for implantable cardioverter defibrillators (ICDs).

Inspired by the successful preparation of $Ag/AgVO_3$ hybrid and their good electrochemical properties, other silver vanadium oxides ($Ag/Ag_2V_4O_{11}$, $Ag/Ag_{0.33}V_2O_5$ and $Ag/Ag_{1.2}V_3O_8$) can also be generally prepared via the same preparation strategy only tuning the molar ratios of Ag to V. According to the XRD results (Supporting information, Figure S7, S8, S9), $Ag_2V_4O_{11}$, $Ag_{0.33}V_2O_5$ and $Ag_{1.2}V_3O_8$ are fabricated at various temperatures. And the XPS results give the evidences of the existence of metallic silver (Ag^0) in the as-prepared Ag/SVOs hybrid including $Ag/Ag_2V_4O_{11}$, $Ag/Ag_{0.33}V_2O_5$ and $Ag/Ag_{1.2}V_3O_8$.

The Ag nanoparticles anchored on silver vanadium oxides (SVOs) are further characterized by Transmission electron microscope (TEM) and the results are shown in Figure 3. As clearly displayed in the TEM images, all the SVOs are uniformly decorated with many small nanoparticles. The SVOs and the individually anchored nanoparticles are further characterized by HRTEM. The

clear lattice fringes with the interplanar spacings of ≈0.237 nm (Figure 3b), ≈0.2056 nm (Figure 3d) and ≈0.323 nm (Figure 3f) correspond well to the distances of (410) of $Ag_2V_4O_{11}$ phase (JCPDS card NO. 49-0166), (204) of $Ag_{0.33}V_2O_5$ phase (JCPDS card NO. 81-1740), and (110) plane of $Ag_{1.2}V_3O_8$ phase (JCPDS card NO. 88-0686), respectively. The HRTEM images of the anchored nanoparticles display the clear lattice fringes, which confirm the existence of silver nanoparticles with a diameter ranging from 2 to 10 nm.

The $Ag_2V_4O_{11}$ material has been commercially used in primary lithium batteries for ICDs because of its high power and long-term (>10 years) stability.[31, 32] In the typical $Ag_2V_4O_{11}$ two-dimensional (2D) layered structure, the Ag^+ ions are located between the layers, and the infinite $[V_4O_{12}]_n$ quadruple strings consisting of two in-equivalent vanadium sites are linked by corner-shared oxygen atoms to provide continuous V–O layers along the (001) plane.[33] In our work, the Ag nanoparticles anchored $Ag_2V_4O_{11}$ electrodes exhibit a relatively high specific capacity of 309 and 272 mA h g^{-1} at 20 and 50 mA g^{-1}, respectively (Supporting information, Figure S10). The electrochemical performance is superior to the rheological phase[6] and hydrothermal method[7] prepared $Ag_2V_4O_{11}$. However, the capacity of $Ag_2V_4O_{11}$ above 3 V is relatively lower when compared to $AgVO_3$ (see Figure S10 and Figure 2). As ICDs work most efficiently above 3 V, so it is importance to achieve higher capacity in high voltage region to improve the performance for ICDs.[11] In this respect, the Ag/$AgVO_3$ hybrid described in this work with superior electrochemical performance may be more suitable as cathode for ICDs.

In respect to $Ag_{0.33}V_2O_5$, with a monoclinic system and space group of $C2/m(12)$, it is composed of V_2O_5 layers and interstitial Ag ions.[34] There are three in-equivalent vanadium sites in the structure of $Ag_{0.33}V_2O_5$, and the V(3) forms infinite zigzag chains to connect the $[V_4O_{11}]_n$ layers

by corner-shared oxygen atoms along the *b*-axis. but in five-fold square pyramidal coordination $V(3)O_5$.[33] The unique crystal structure is different from the 2D layered structure of $Ag_2V_4O_{11}$ and results in the 3D tunneled structure of $Ag_{0.33}V_2O_5$. Compared to $Ag_2V_4O_{11}$ and $AgVO_3$, $Ag_{0.33}V_2O_5$ is much more stable during lithiation and delithiation process because the novel 3D tunneled structure can alleviate structural collapse and crystallinity loss. Therefore, among the silver vanadium oxides (SVOs), $Ag_{0.33}V_2O_5$ material is the most possible for being used as cathode material in rechargeable lithium batteries. The electrochemical performances of $Ag/Ag_{0.33}V_2O_5$ hybrid as cathode materials in rechargeable lithium batteries are evaluated. Initial cyclic voltammogram (CV) curve displays four cathodic peaks and four anodic peaks, indicating the multi-step intercalation/deintercalation of the lithium ions, which is in good agreement with the discharge/change curves with four distinct plateaus observed at about 3.3 V, 3.0 V, 2.5 V and 2.0 V (Supporting information, Figure S11). Figure 4a shows the cycling performance of $Ag/Ag_{0.33}V_2O_5$ hybrid at 100 mA g^{-1}. High initial specific capacity of 220 mA h g^{-1} can be obtained for $Ag/Ag_{0.33}V_2O_5$ electrode and 194 mA h g^{-1} is maintained after 50 cycles, with the capacity retention of 88%. Long-term cycling performance (Figure 4b) indicates that the hybrid exhibits high specific capacity of 137 mA h g^{-1} at 300 mA g^{-1}, and 132 mA h g^{-1} still can be retained after 200 cycles, corresponding to 96.4 % of its initial capacity, which is amazing for the SVOs electrodes. What's more, high coulombic efficiency around 99% can be reached. Recent studies have demonstrated good retrievability that the crystal structure of the initial $Ag_{0.33}V_2O_5$ can be recovered after several cycles.[6, 35] The integrity of the crystal structure of $Ag_{0.33}V_2O_5$ can be remained even after 50 cycles (Supporting information, Figure S12). Therefore, the superior electrochemical performance of $Ag/Ag_{0.33}V_2O_5$ hybrid is attributed to the good structural reversibility and the enhanced conductivity

with introduction of Ag nanoparticles.

As a typical layered structure of $Ag_{1+x}V_3O_8$, it is isostructural with $Li_{1+x}V_3O_8$ in a monoclinic system with the space group of $P2_1/m$.[1] In the $Ag_{1+x}V_3O_8$ layered structure, the $[V_3O_8]_n$ framework is built up around three independent vanadium sites with two octahedrally coordinated and one trigonal-bipyramidal coordination containing two structural units with a double chain of edge-shared trigonal bipyramids connecting the double chains of edge-shared VO_6 octahedra infinite along the [010] direction, and the Ag^+ ions mainly reside in weakly distorted octahedral sites, which due to the main Li^+ ion sites observed in $Li_{1.2}V_3O_8$.[7, 36] During the electrochemical lithiation process, the Ag^+ in $Ag_{1.2}V_3O_8$ structure will continuously deposit on the surface of the active material as metallic silver anchored, and the metallic silver is not inserted into the layers during the following lithiation and delithiation process.[15, 37] In our recently study, we found that the Li^+ ions may replace the Ag^+ ions at the octahedral sites in $Ag_{1.2}V_3O_8$ to form $Li_{1+x}V_3O_8$, and this structure is reversible upon cycling, which is confirmed by the *ex-situ* XRD for the electrodes after discharge/charge process.[15] The superior cycling performance of $Ag_{1.2}V_3O_8$ over $AgVO_3$ can be attributed to the good structural stability of $Li_{1+x}V_3O_8$ formed after fist discharge process. The $Ag/Ag_{1.2}V_3O_8$ hybrid is first time reported and their cycling performance evaluated at 100 mA g^{-1} is displayed in Figure 4c. A high initial discharge capacity of 246 mA h g^{-1} can be achieved for the electrode, which decreases to 190 mA h g^{-1} at the second cycle. This may due to the successive phase transformations upon lithium ion insertion into $Ag_{1.2}V_3O_8$, forming the new phase of metallic Ag^0 and $Li_{1+x}V_3O_8$.[15] A stabilized specific discharge capacity of 164 mA h g^{-1} can be obtained after 50 cycles. The good performance is ascribed to the good structural stability of the forming $Li_{1+x}V_3O_8$.

Silver vanadium oxides (SVOs), including $AgVO_3$, $Ag_2V_4O_{11}$, $Ag_{0.33}V_2O_5$ and $Ag_{1.2}V_3O_8$, have obtained by a general strategy in this work. In the past few years, $AgVO_3$ and $Ag_2V_4O_{11}$ materials are generally investigated as cathode for primary lithium batteries, while $Ag_{0.33}V_2O_5$ and $Ag_{1.2}V_3O_8$ for rechargeable lithium batteries. This is because irreversible phase transformation and formation of amorphous phase after first cycle for $AgVO_3$ and $Ag_2V_4O_{11}$, leading to the unsatisfactory cyclic behavior.[11, 12] However, $Ag_{0.33}V_2O_5$ demonstrates the excellent structural stability and $Ag_{1.2}V_3O_8$ transfers to the good structural stability phase of $Li_{1+x}V_3O_8$, which make them potential cathode for LIBs.[6, 15, 37] As is showed in Table S2, the Ag/$AgVO_3$ and Ag/$Ag_2V_4O_{11}$ exhibit high initial discharge capacity and good rate capability, especially for Ag/$AgVO_3$, high specific discharge capacity of 199 mA h g^{-1} can be achieved even at an ultra-high discharge current density of 5 A g^{-1}, which is desirable for ICDs. While for Ag/$Ag_{0.33}V_2O_5$ and Ag/$Ag_{1.2}V_3O_8$ electrodes, although lower initial discharge capacities are observed at different current densities, they show good cyclic stability, and the results are superior to $Ag_{0.33}V_2O_5$ nanowires,[6] $Ag_{0.33}V_2O_5$ nanorods,[14] and channel-structured $Ag_{0.33}V_2O_5$ nanorods,[38] and belt-like $Ag_{1.2}V_3O_8$,[15] respectively.

In summary, a general strategy has been reported for the one-pot synthesis of Ag nanoparticles uniformly anchored on a series of silver vanadium oxides (SVOs), such as Ag/$AgVO_3$, Ag/$Ag_2V_4O_{11}$, Ag/$Ag_{0.33}V_2O_5$ and Ag/$Ag_{1.2}V_3O_8$. The as-obtained Ag/SVOs hybrids have demonstrated the highly improved electrochemical properties because of the enhanced electron conductivity. For example, the Ag/$AgVO_3$ hybrid exhibits excellent rate capability: a high specific discharge capacity of 199 mA h g^{-1} can be reached at an ultra-high discharge current density of 5 A g^{-1}. In particular, this method is cost-effective, environmental benign and large scale production available. It is believed that our strategy could be probably applicable for the preparation of other

metal vanadium oxides with great promise for various applications.

Acknowledgements

This work was supported by the National High Technology Research and Development Program of China (863 Program) (Grant no. 2013AA110106), the National Natural Science Foundation of China (Grant no. 51374255), the Lie-Ying Program of Central South University and the Hunan Provincial Innovation Foundation For Postgraduate.

Notes and references

1. K. J. Takeuchi, A. C. Marschilok, S. M. Davis, R. A. Leising and E. S. Takeuchi, *Coord. Chem. Rev.,* 2001, **219-221**, 283-310.
2. J. M. Song, Y. Z. Lin, H. B. Yao, F. J. Fan, X. G. Li and S. H. Yu, *ACS Nano,* 2009, **3**, 653-660.
3. C. Han, Y. Pi, Q. An, L. Mai, J. Xie, X. Xu, L. Xu, Y. Zhao, C. Niu, A. M. Khan and X. He, *Nano Lett.,* 2012, **12**, 4668-4673.
4. F. Sauvage, V. Bodenez, J. M. Tarascon and K. R. Poeppelmeier, *J. Am. Chem. Soc.,* 2010, **132**, 6778-6782.
5. M. R. Parida, C. Vijayan, C. S. Rout, C. S. Suchand Sandeep and R. Philip, *Appl. Phys. Lett.,* 2012, **100**, 121119.
6. W. Hu, X. B. Zhang, Y. L. Cheng, C. Y. Wu, F. Cao and L. M. Wang, *ChemSusChem,* 2011, **4**, 1091-1094.
7. C. Wu, H. Zhu, J. Dai, W. Yan, J. Yang, Y. Tian, S. Wei and Y. Xie, *Adv. Funct. Mater.,* 2010,

20, 3666-3672.

8. L. Mai, L. Xu, Q. Gao, C. Han, B. Hu and Y. Pi, *Nano Lett.,* 2010, **10**, 2604-2608.

9. R. A. Leising and E. S. Takeuchi, *Chem. Mater.,* 1994, **6**, 489-495.

10. L. Mai, X. Xu, C. Han, Y. Luo, L. Xu, Y. A. Wu and Y. Zhao, *Nano Lett.,* 2011, **11**, 4992-4996.

11. S. Zhang, W. Li, C. Li and J. Chen, *J. Phys. Chem. B,* 2006, **110**, 24855-24863.

12. S. Liang, J. Zhou, A. Pan, X. Zhang, Y. Tang, X. Tan, T. Chen and R. Wu, *J. Power Sources,* 2013, **228**, 178-184.

13. S. Liang, J. Zhou, X. Zhang, Y. Tang, G. Fang, T. Chen and X. Tan, *CrystEngComm,* 2013, **15**, 9869-9873.

14. Y. Wu, P. Zhu, X. Zhao, M. V. Reddy, S. Peng, B. V. R. Chowdari and S. Ramakrishna, *J. Mater. Chem. A,* 2013, **1**, 852-859.

15. S. Liang, T. Chen, A. Pan, J. Zhou, Y. Tang and R. Wu, *J. Power Sources,* 2013, **233**, 304-308.

16. E. S. Takeuchi, A. C. Marschilok, K. Tanzil, E. S. Kozarsky, S. Zhu and K. J. Takeuchi, *Chem. Mater.,* 2009, **21**, 4934-4939.

17. C. Lu, Q. Shen, X. Zhao, J. Zhu, X. Guo and W. Hou, *Sensor. Actuat. B-Chem.,* 2010, **150**, 200-205.

18. R. D. Holtz, A. G. Souza Filho, M. Brocchi, D. Martins, N. Duran and O. L. Alves, *Nanotechnology,* 2010, **21**, 185102.

19. M. W. Shao, L. Lu, H. Wang, S. Wang, M. L. Zhang, D. D. Ma and S. T. Lee, *Chem. Commun.,* 2008, 2310-2312.

20. Z. Chen, S. Gao, R. Li, M. Wei, K. Wei and H. Zhou, *Electrochim. Acta*, 2008, **53**, 8134-8137.

21. R. D. Holtz, B. A. Lima, A. G. Souza Filho, M. Brocchi and O. L. Alves, *Nanomed. Nanotechnol. Biol. Med.,* 2012, **8**, 935-940.

22. F. Cheng and J. Chen, *J. Mater. Chem.,* 2011, **21**, 9841.

23. S. Kittaka, K. Matsuno and H. Akashi, *J. Solid State Chem.,* 1999, **142**, 360-367.

24. P. Rozier, J. M. Savariault and J. Galy, *J. Solid State Chem.,* 1996, **122**, 303-308.

25. A. C. Marschilok, E. S. Kozarsky, K. Tanzil, S. Zhu, K. J. Takeuchi and E. S. Takeuchi, *J. Power Sources,* 2010, **195**, 6839-6846.

26. E. S. Takeuchi, A. C. Marschilok, K. J. Takeuchi, A. Ignatov, Z. Zhong and M. Croft, *Energy Environ. Sci.,* 2013, **6**, 1465-1470.

27. Y. K. Anguchamy, J. W. Lee and B. N. Popov, *J. Power Sources*, 2008, **184**, 297-302.

28. J. W. Lee and B. N. Popov, *J. Power Sources*, 2006, **161**, 565-572.

29. L. Liang, H. Liu and W. Yang, *Nanoscale,* 2013, **5**, 1026-1033.

30. S. Zhang, S. Peng, S. Liu, L. Ren, S. Wang and J. Fu, *Mater. Lett.,* 2013, **110**, 168-171.

31. C. L. Schmidt and P. M. Skarstad, *J. Power Sources,* 2001, **97-98**, 742-746.

32. A. M. Crespi, S. K. Somdahl, C. L. Schmidt and P. M. Skarstad, *J. Power Sources,* 2001, **96**, 33-38.

33. Y. Xu, X. Han, L. Zheng, W. Yan and Y. Xie, *J. Mater. Chem.,* 2011, **21**, 14466.

34. Y. Liu, Y. Zhang, M. Zhang and Y. Qian, *J. Cryst. Growth,* 2006, **289**, 197-201.

35. S. Liang, Y. Yu, T. Chen, A. Pan, S. Zhang, J. Zhou, Y. Tang and X. Tan, *Mater. Lett.,* 2013, **109**, 92-95

36. P. Rozier, and J. Galy, *J. Solid State Chem.,* 1997, **134**, 294-301.

37. J. Kawakita, Y. Katayama, T. Miura and T. Kishi, *Solid State Ionics,* 1997, **99**, 71-78.

38. S. Liang, X. Zhang, J. Zhou, J. Wu, G. Fang, Y. Tang and X. Tan, *Mater. Lett.,* 2014, **116**, 389-392.

Figures and Captions

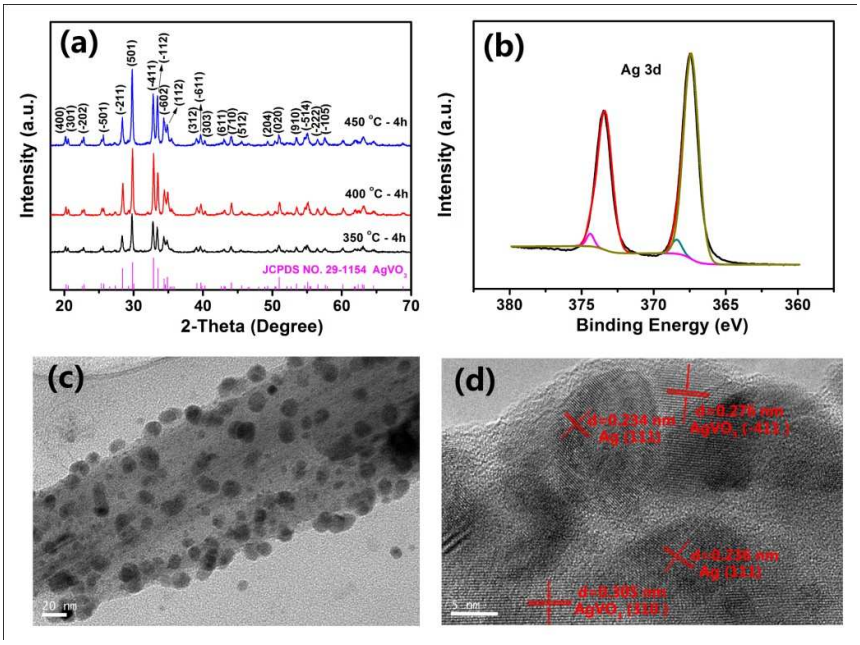

Figure 1. (a) XRD patterns of Ag/$AgVO_3$ hybrids prepared at different temperatures; (b) X-ray photoelectron spectroscopy of Ag 3d states in Ag/$AgVO_3$ hybrid obtained at 400 ^{o}C for 4h; (c) TEM image and (d) HRTEM of an individual Ag/$AgVO_3$ nanorod prepared at 400 ^{o}C for 4h.

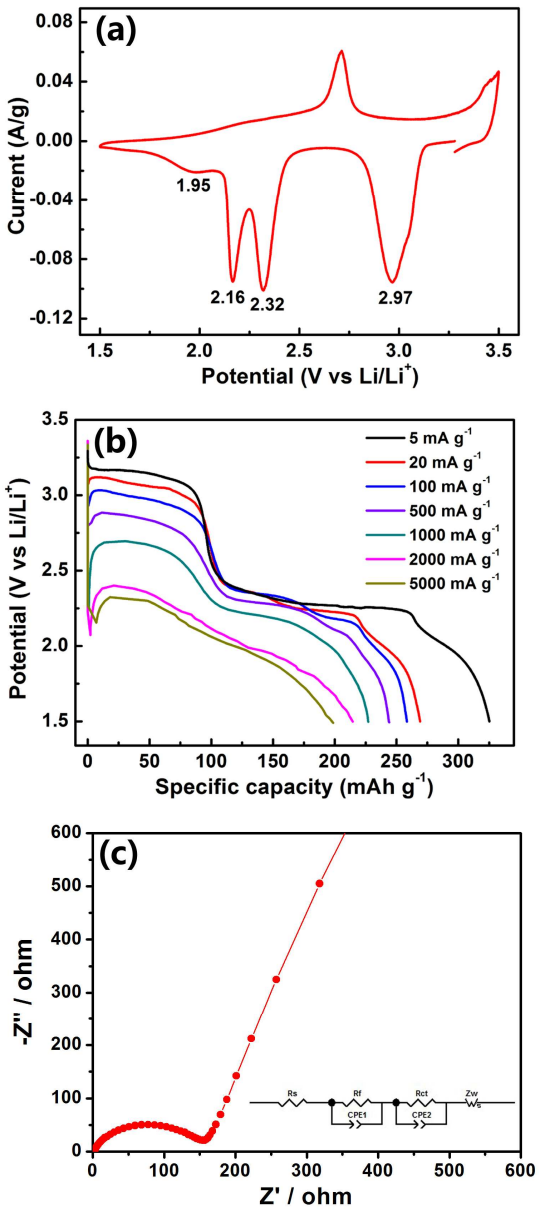

Figure 2. (a) Initial cyclic voltammetry (CV) curve, (b) initial discharge curves at different current densities and (c) nyquist plot of Ag/$AgVO_3$ hybrid prepared at 400 ^{o}C for 4h, respectively. Inset (c) shows the equivalent circuit model for the impedance spectra.

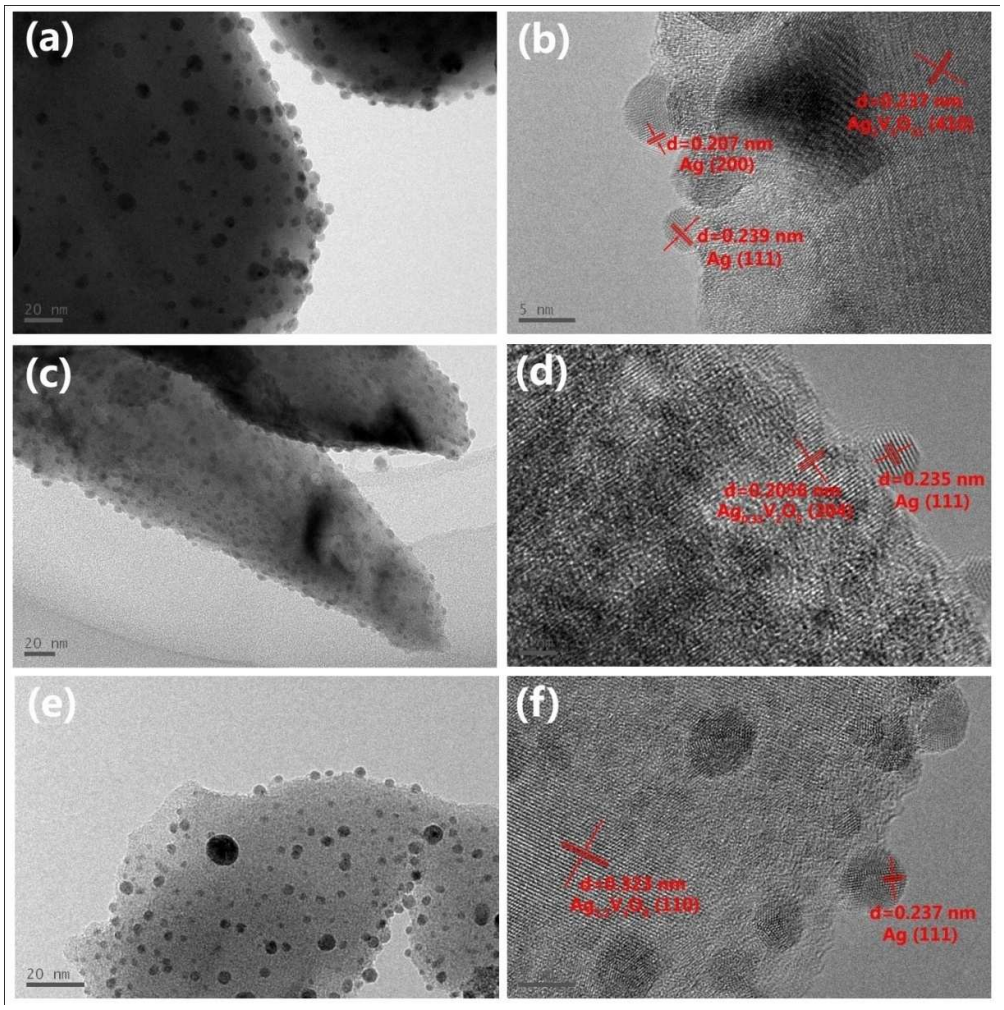

Figure 3. TEM images and the corresponding HRTEM images of the Ag/SVOs hybrids: (a, b) $Ag/Ag_2V_4O_{11}$ prepared at 500 ^oC for 2h; (c, d) $Ag/Ag_{0.33}V_2O_5$ prepared at 450 ^oC for 4h and (e, f) $Ag/Ag_{1.2}V_3O_8$ hybrid prepared at 450 ^oC for 4h, respectively.

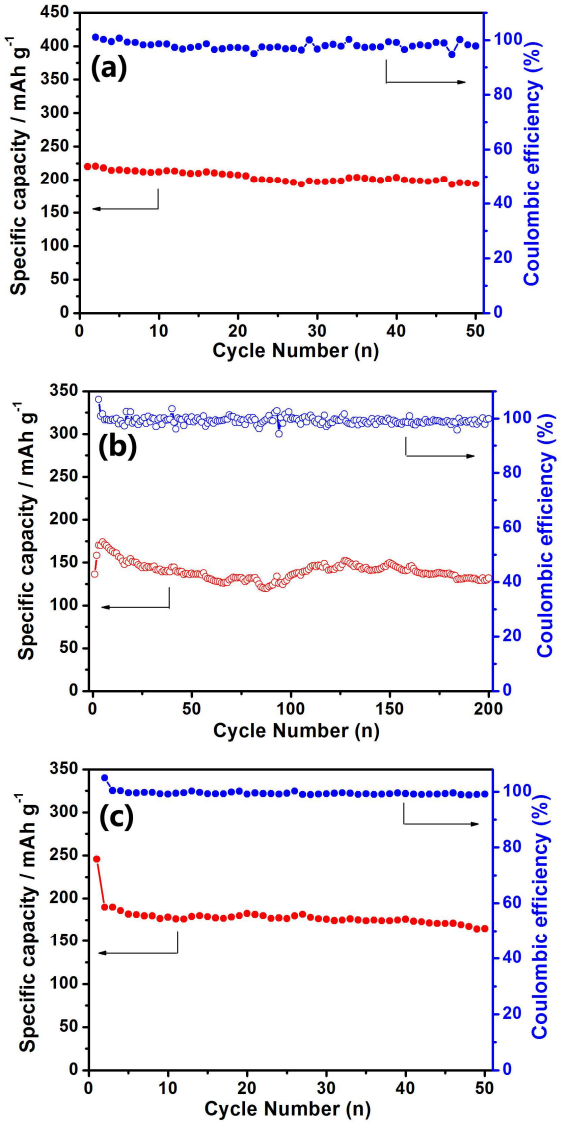

Figure 4. (a, b) Cycling performance of $Ag/Ag_{0.33}V_2O_5$ hybrid prepared at 450 ^oC for 4h at the current densities of 100 mA g^{-1} and 300 mA g^{-1}, respectively. (c) Cycling performance of $Ag/Ag_{1.2}V_3O_8$ hybrid prepared at 450 ^oC for 4h at the current density of 100 mA g^{-1}.

Graphical Abstract

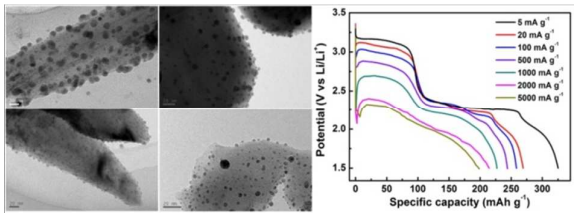

A general approach has been developed to synthesis a series of silver vanadium oxides (SVOs) anchored with Ag nanoparticles, including $AgVO_3$, $Ag_2V_4O_{11}$, $Ag_{0.33}V_2O_5$ and $Ag_{1.2}V_3O_8$, which exhibit highly improved electrochemical performances.